Journal of Engineering Mathematics **34:** 335–357, 1998.

An asymptotic description of the attached, turbulent, oscillatory boundary layer

M. J. BUTLER[1], P. W. DUCK[1] and P. K. STANSBY[2]
[1]*Department of Mathematics, The University, Manchester M13 9PL, UK*
[2]*Hydrodynamics Research Group, Manchester School of Engineering, The University, Manchester M13 9Pl, UK*

Received 15 December 1997; accepted in revised form 22 June 1998

Abstract. The attached, temporally-oscillating turbulent boundary layer is investigated by use of asymptotic matching techniques, valid for the limit of large Reynolds numbers. Much of the analysis is applicable to generally accepted turbulence models (which satisfy a few basic assumptions as detailed in the paper), and this is then applied in particular to two well established turbulence models, namely the $k-\varepsilon$ transport model and the Baldwin–Lomax mixing-length model. As in the laminar case, the steady-streaming Reynolds number is found to be an important parameter, although in the turbulent case this is important at leading (rather than second) order. In particular, the time dependence of the wall shear (and the displacement thickness) is found to leading order to be independent of the specific closure model, but just differs by a multiplicative constant dependent on the particular model. Results are also compared with previous computational and experimental data; the agreement is encouraging.

In addition to describing the oscillatory flow above a flat wall, these leading order results are applicable to flow past general bodies, provided the amplitude of oscillation is small compared to the surface radius of curvature. In the case of the Baldwin–Lomax model, the nature of the higher-order terms, including the steady streaming caused by the interaction of curvature and inertia effects is also investigated. This analysis suggests some limitations on the applicability of the model to the finer details of the flow, due to the occurrence of discontinuities (and singularities) in the higher-order asymptotic solution, particularly when inertia effects are taken into account.

Keywords: oscillatory, turbulent boundary layers, asymptotics, very high Reynolds number flows.

1. Introduction

Analytical solutions for oscillatory laminar boundary layers are well known (Stokes [1]); at high enough Reynolds number the boundary layers become turbulent and investigations have been made through physical experiment, *e.g.* Jensen *et al.* [2], and direct numerical simulation, *e.g.* Spalart and Baldwin [3]. Numerical solutions of the Reynolds-averaged Navier-Stokes equations with various levels of turbulence model have also been made, *e.g.* Fredsoe [4], Justesen and Spalart [5], Cobbin *et al.* [6]. In this paper we will derive some analytical solutions for these equations.

A general problem is first posed to leading order based on two well-established near-wall properties of turbulent boundary layers and the quasi-steady assumption. Two widely used turbulence models based on the eddy viscosity concept are then considered in detail: the $k-\varepsilon$ transport model (k is turbulence energy and ε its dissipation rate, Jones and Launder [7]) and the Baldwin–Lomax mixing-length model (Baldwin and Lomax [8]). Results for sinusoidal flow over a (smooth) flat plate are derived and compared with experimental and numerical data. The flat-plate results may also be applied to small-amplitude, but high Reynolds number, oscillatory flow about a general cylinder by considering the boundary layer on its surface to

be equivalent to a series of flat-plate boundary-layer problems defined by the local Reynolds number (following Cobbin *et al.* [6]).

This problem for laminar flow was first solved, quite generally, to leading order by Stokes [1] who derived the viscous damping force (the force component in phase with velocity). Stuart [9] and Riley [10, 11] found the flow to be dependent on two Reynolds numbers

$$\mathrm{Re} = \frac{\omega a^2}{\nu}, \tag{1}$$

and the so-called steady-streaming Reynolds number, given by

$$\mathrm{Rs} = \delta^2\,\mathrm{Re} = \frac{U_\infty^{*2}}{\omega\nu}, \tag{2}$$

with

$$\delta = \frac{U_\infty^*}{\omega a}, \tag{3}$$

where U_∞^* is the amplitude of the external flow velocity, and δ is an amplitude parameter, and is a measure of the ratio of the amplitude of fluid particle oscillation compared with a body scale a. When both Reynolds numbers are large the laminar flow exhibits a double-layer structure, with a thin inner layer of thickness $O((\nu/\omega)^{1/2})$ where the flow is predominantly oscillatory, and a much thicker outer layer of thickness $O(\mathrm{Rs}^{-1/2}a)$ in which the velocity decays to that of the freestream. In particular it is found that the flow exhibits a steady-streaming component, induced by the Reynolds stresses of the oscillatory flow. There is bulk movement of fluid from the top and bottom of the cylinder towards the line parallel to the flow oscillation through the centre of the cylinder. This steady streaming thus produces two jets, one on either side of the cylinder, along this line of symmetry. The form of the steady streaming is strongly influenced by the parameter Rs. In this paper some analysis to higher order will be made with the Baldwin–Lomax turbulence model.

While these flows have clearly long been of fundamental interest, they are also of considerable practical importance. The periodic boundary layer induced on the sea bed due to the passage of surface waves causes wave attenuation and possibly sediment movement (although the rough-bed conditions normally encountered will be the subject of further study). The viscous damping force on cylinders of various shape, at very high Reynolds numbers, is a significant factor in the design of deep-water (dynamically constrained) offshore structures, notably the tension-leg patform. Although the analysis here is for attached boundary layers, this is important in certain cases and, when separation does occur, an attached-flow damping estimate would still give a useful lower-bound estimate.

Experimental work on small amplitude oscillatory flows around cylinders has been carried out by Keulegan and Carpenter [12] and Sarpkaya [13, 14]. The transition of Stokes layers on cylinders from the laminar to turbulent state was studied experimentally by Honji [15] and theoretically by Hall [16]. In most practical situations the flow is predominantly turbulent.

Here we use asymptotic matching techniques valid in the limit $\mathrm{Rs} \to \infty$ in place of previous numerical methods, although we use the latter (together with experimental results) to validate our results. The eddy-viscosity concept has been widely used in earlier studies; by introducing the fluctuating turbulent quantities into the boundary-layer equations and taking mean quantities in an averaging time which is small in relation to the oscillation period, the

boundary-layer equation involving Reynolds stresses is obtained. According to the Boussinesq assumption these stresses are related to the mean velocity gradients through a turbulent or eddy viscosity, ν_t^*, which must be specified through a turbulence model.

Kajiura [17] made one of the first solution attempts, in which the eddy viscosity was assumed constant in a small inner layer, varied linearly with distance from the bed in an intermediate region, and was constant above a certain distance from the bed. He obtained a lengthy analytical-numerical solution. By avoiding the use of the inner layer, Brevik [18] simplified Kajiura's calculations although he (like Kajiura) did not take into account that eddy viscosity could be a function of time as well as distance from the wall. Bakker [19] adopted a mixing-length hypothesis, after that of Prandtl [20], in which the mixing length was proportional to the distance from the bed, but he did not allow the eddy viscosity to decay at large distances from the bed. Fredsoe [4] used the approach of Jonnson and Carlsen [21] assuming the velocity to vary logarithmically, obtaining analytic results for both smooth and rough beds. Direct numerical solution was undertaken by Spalart and Baldwin [3] for flow in and beyond the transition region. Justesen and Spalart [5] performed numerical computations using the $k-\varepsilon$ eddy viscosity model, together with a near-wall function for the velocity. Experimental work has been carried out for smooth and rough beds by Jensen *et al.* [2]. We shall be comparing the present results with those from some of these later papers.

To analyse the oscillatory flow over a general, nonplanar surface, we consider an orthogonal coordinate system $a(s, n)$, with s, n denoting the nondimensional tangential and normal coordinates respectively; the corresponding velocity vector is taken to be $U_\infty^*(u, v)$, where the freestream flow is taken to be $U_\infty^* \cos \omega t^*$ (although it is trivial to generalise this to general periodic temporal forms with zero mean, as carried out in Section 5). We then assume that potential theory provides a flow on the wall surface given by

$$(u, v) = (U(s) \cos t, 0). \tag{4}$$

Further nondimensionalisation is carried out by writing

$$t = \omega t^*, \qquad \nu_e^* = \nu^* \nu_e, \qquad p^* = a U_\infty^* \omega \rho^* p, \tag{5}$$

where ν^* and ρ^* are the dimensional laminar viscosity and density respectively (both assumed constant); the resulting boundary-layer equations are given by

$$\frac{\partial u}{\partial t} + \delta \left(u \frac{\partial u}{\partial n} + u \frac{\partial u}{\partial s} \right) = -\frac{\partial p}{\partial s} + \frac{1}{\mathrm{Re}} \frac{\partial}{\partial n} \left(\nu_e \frac{\partial u}{\partial n} \right), \tag{6}$$

$$\frac{\partial p}{\partial n} = 0, \tag{7}$$

$$\frac{\partial v}{\partial n} + \frac{\partial u}{\partial s} = 0. \tag{8}$$

Here $\nu_e = 1 + \nu_t$ is the nondimensional effective viscosity, and ν_t the nondimensional eddy viscosity. We now make two basic assumptions, $\delta \ll 1$ (corresponding to small amplitude oscillations), and $\mathrm{Re} \gg 1$ (and, indeed, the stronger requirement $\mathrm{Rs} \gg 1$). The first assumption (which implies fluid particle oscillations much smaller than the scale of the body is clearly not necessary in the case of flow over a flat plate) allows a certain amount of progress to be made

with the equations using linearisation (just as in the laminar case), while the second gives the region of most practical use (and is also the most interesting area mathematically).

Some previous work has been carried out using asymptotic matching techniques for *steady* turbulent flows in pipes, channels and two-dimensional boundary layers by Yajnik [22], Mellor [23] and Bush and Fendell [24]. They found the flow consisted of distinct regions, an inner viscous layer, a defect layer and an outer potential flow (in the case of external flows). Yajnik [22] solved an under-determined system of equations using asymptotic hypotheses to obtain the velocity defect law and the logarithmic law of the wall. He hypothesized that in the inner layer the production of turbulent kinetic energy by the mean flow was of the same order as the diffusion due to the fluctuating motion. In the outer layer the Reynolds stresses alone were assumed to remain significant. Mellor [23] repeated some of Yajnik's analysis but without assuming details of the asymptotic behaviour of the Reynolds stresses at the outer edge of the inner, viscous layer. He too obtained the law of the wall and the velocity defect law, and investigated the smaller scale structure by use of a two-point velocity correlation, and found the two-thirds power law in velocity correlation space. Bush and Fendell [24] used an algebraic eddy-viscosity as a closure to solve for channel and two-dimensional boundary-layer flows, and obtained the law of the wall and the velocity defect law. They assumed the turbulent and laminar stresses balanced in the inner layer, whilst the turbulent stress balances the convection of momentum in the outer layer. They also used a differential relationship for the eddy viscosity in the case of channel flows to emphasize history effects and found it only made minor changes to the solution. This work was extended by He *et al.* [25] to compressible turbulent boundary layers. As before the flow exhibits a two-layer structure. They found the flow obeyed the law of the wall in the overlap region of the two layers, and they formulated algebraic turbulence models to take into account compressibility in the outer layer. Degani *et al.* [26] and [27] have studied the large Reynolds number limit of attached steady three-dimensional turbulent boundary layers also by the use of asymptotic methods. They found the flow has a two-layer structure as before, with the law of the wall valid in the overlap region of the two layers. They also found the flow in the inner layer is equivalent to two-dimensional flow to leading order, with no crosswise velocity at this order. Additionally, Neish and Smith [28] considered turbulent separation of the flow past a bluff body, again using asymptotic methods, together with a degree of turbulence modelling (the limitations of which have also been discussed).

This paper is concerned with asymptotic analysis of the above oscillatory problem in the limit as $\mathrm{Rs} \to \infty$. First (Section 2) we present a leading order solution to the problem, valid for generally accepted turbulence models. This solution also serves to describe the fundamental problem of turbulent, oscillatory flow over a flat plate (together with flow over nonplanar surfaces, provided the amplitude of oscillation is relatively small), and as such is directly analogous to the classical Stokes solution applicable to laminar flows. Next, in Section 3 the particular details for the well-known $k - \varepsilon$ transport model are given, whilst in Section 4 analysis for the somewhat simpler Baldwin–Lomax mixing-length model is considered; in this section higher-order effects are also discussed, including some details of the steady streaming which is produced through nonlinear effects. In Section 5 various numerical results obtained from the analyses are presented, and compared with previous numerical and experimental results; we also include our conclusions in this section.

2. Leading-order solution

Generally acceptable turbulence models tend to lead to a number of common flow characteristics (not least of which is the well-known log law). We exploit the general features of these models by making (a few) general, basic assumptions regarding these models.

We start by introducing the scaled radial length scale

$$Y = n\,\mathrm{Re}^{1/2}. \tag{9}$$

In the case of laminar flows the scale $Y = O(1)$ is the most significant; although laminar flows are not central to our interests here (and, indeed this turns out not to be a crucial scale in the asymptotic analysis of turbulent boundary layers), nonetheless this scale serves as a useful starting point for our analysis.

We then suppose the flow to develop as follows

$$u = u_0(Y, s, t) + \delta u_1(Y, s, t) + O(\delta^2), \tag{10}$$

$$v = \mathrm{Re}^{-1/2}[\delta v_1(Y, s, t) + O(\delta^2)]. \tag{11}$$

Thus to leading order (6) becomes

$$\frac{\partial u_0}{\partial t} = -U \sin t + \frac{\partial}{\partial Y}\left(\nu_e \frac{\partial u_0}{\partial Y}\right), \tag{12}$$

where, in the case of flow past a circular cylinder $U = 2\sin s$, whilst for a flat plate $U = 1$; here our only requirement is that $U = U(s)$. The boundary conditions become

$$u_0 \to U\cos t \quad \text{as } Y \to \infty, \tag{13}$$

and

$$u_0 = 0 \quad \text{on } Y = 0. \tag{14}$$

The details of the particular turbulence model are (implied to be) contained exclusively within the effective viscosity ν_e. Ignoring (for the present) the lower portion of the near wall/sublayer region we make the entirely reasonable assumptions that

(i) the shear stress varies negligibly over the near-wall region,
(ii) the flow is quasi-steady in this region and
(iii) the eddy viscosity takes the Prandtl–van Driest form, basically (62) below, with the mixing length l being proportional to the distance from the wall Y (later this condition will be relaxed slightly, but it serves as a helpful initial assumption).

Assumptions (i) and (ii) are basic properties assumed in most turbulent boundary-layer studies, but may also be verified *a posteriori* in our asymptotic results.

The immediate implication of (iii) is that we may write the nondimensional eddy viscosity in the form

$$\nu_t = \mathrm{Rs}^{1/2}\lambda_1^2 Y^2 \left|\frac{\partial u_0}{\partial Y}\right|, \tag{15}$$

where λ_1 is a constant (this may be shown to be $O(1)$ in both the models later taken). We note already the occurrence of the parameter Rs, the so-called steady-steaming Reynolds number, as given by (2). This parameter turns out to be fundamental in determining the nature of the turbulent flow, and will be used extensively in what follows. In the laminar case, this parameter is also of some significance, but only with regard to the higher order, steady streaming. In the turbulent case, in the limit $\mathrm{Rs} \to \infty$, we find a double-layer structure again; this also occurs in the laminar case, although the details turn out to be very different. In particular, in the laminar case the leading order boundary-layer flow involves just one scale and the outer region is only of significance to the higher-order steady streaming. In the turbulent case, the sublayer is dominated by viscous effects and the flow is relatively slow compared with the outer flow. We scale the tangential velocity and normal length scale according to

$$u_0 = \delta_1 \tilde{u}_0, \qquad Y = \delta_2 \widetilde{Y}, \tag{16}$$

where we assume $\tilde{u}_0, \widetilde{Y} = O(1)$, and $\delta_1, \delta_2 \ll 1$. Consequently, this implies a layer somewhat thinner than that which occurs in laminar (Stokes) flows. In terms of these new variables, we now have (utilising (15))

$$(\nu_e)_{\text{inner}} = 1 + \lambda_1^2 \,\mathrm{Rs}^{1/2} \delta_1 \delta_2 \left| \frac{\partial \tilde{u}_0}{\partial \widetilde{Y}} \right| \widetilde{Y}^2. \tag{17}$$

If the eddy and laminar viscosities are comparable (as indeed they must be in the sublayer), then we have

$$\delta_1 \delta_2 \,\mathrm{Rs}^{1/2} = O(1). \tag{18}$$

The boundary-layer equation (6) becomes quasi-steady to leading order,

$$\frac{\partial}{\partial \widetilde{Y}} \left(\nu_e \frac{\partial \tilde{u}_0}{\partial \widetilde{Y}} \right) = 0, \tag{19}$$

consistent with assumption (ii) above. We note from (12), that the terms contained in (19) are $O(\delta_1^3 \,\mathrm{Rs})$, which is somewhat larger than the pressure gradient term which is $O(1)$. On integrating this expression once, we obtain

$$\frac{\partial \tilde{u}_0}{\partial \widetilde{Y}} = \frac{K(t,s)}{1 + \lambda_1^2 \widetilde{Y}^2 \left| \frac{\partial \tilde{u}_0}{\partial \widetilde{Y}} \right|}, \tag{20}$$

where $K(t,s)$ is an, as yet, undetermined function.

If we define for convenience

$$\kappa = \mathrm{sign} \left\{ \frac{\partial \tilde{u}_0}{\partial \widetilde{Y}} \right\}, \tag{21}$$

then in the limit $\widetilde{Y} \to \infty$

$$\tilde{u}_0 \to \kappa \frac{\sqrt{\kappa K(t,s)}}{\lambda_1} \log \widetilde{Y}. \tag{22}$$

Note here how the well-known log law emerges quite naturally from the analysis (partly as a consequence of the basic assumptions).

For the outer layer where the velocity approaches the free-stream velocity, to leading order we define the appropriate scale to be $\tilde{y} = \delta_3 Y$, and assuming $\delta_3 \ll 1$, we write

$$u_0 = U\cos t + \delta_1 u_0^*(\tilde{y}, s, t) + \cdots. \tag{23}$$

If we now assume

$$\frac{\delta_1\,\mathrm{Rs}^{1/2}}{\delta_3} \gg 1, \tag{24}$$

the leading order momentum equation may be written

$$\frac{\partial u_0^*}{\partial t} = \delta_1\delta_3\,\mathrm{Rs}^{1/2}\frac{\partial}{\partial\tilde{y}}\left(\nu_e\frac{\partial\tilde{u}_0^*}{\partial\tilde{y}}\right), \tag{25}$$

where the eddy viscosity is given by

$$(\tilde{\nu}_e)_{\text{inner}} = \lambda_1^2\left|\frac{\partial\tilde{u}_0^*}{\partial\tilde{y}}\right|\tilde{y}^2, \tag{26}$$

and therefore a sensible balancing of terms demands that

$$\delta_3^{-1} = \delta_1\,\mathrm{Rs}^{1/2}, \tag{27}$$

(and so $\delta_3 = \delta_2$). The equation to be solved in the outer layer then reduces to

$$\frac{\partial u_0^*}{\partial t} = \frac{\partial}{\partial\tilde{y}}\left(\tilde{\nu}_e\frac{\partial u_0^*}{\partial\tilde{y}}\right), \tag{28}$$

with boundary conditions

$$u_0^* \to 0 \quad \text{as } \tilde{y}\to\infty \tag{29}$$

and

$$u_0^* \to \kappa\frac{\sqrt{\kappa K}}{\lambda_1}\log\tilde{y} = U\cos t\log\tilde{y} \quad \text{as } \tilde{y}\to 0. \tag{30}$$

This equality arises from the matching of (22) and (23), and so

$$U\cos t = \kappa\frac{\sqrt{\kappa K(t,s)}}{\lambda_1}\delta_1\log(\delta_1^2\,\mathrm{Rs}), \tag{31}$$

giving

$$K(t,s) = \lambda_1^2 U\cos t|U\cos t|. \tag{32}$$

Taking the sign of (30), we require

$$\kappa = \mathrm{sign}\{U\cos t\} \tag{33}$$

and we also impose the condition to ensure proper matching

$$\delta_1 \log(\delta_1^2 \,\mathrm{Rs}) = 1, \tag{34}$$

(although later this condition will be modified slightly to take into account higher-order effects). Equation (34) represents a transcendental link between δ_1 and Rs. Such relationships have been found before, for example in the context of axisymmetric viscous flows (Duck, [29]). The equation can be solved by iteration/successive approximation. For example, a first approximation is

$$\delta_1 = \frac{1}{\log\ \mathrm{Rs}}, \tag{35}$$

with a second approximation being

$$\delta_1 \frac{1}{\log\ \mathrm{Rs} - 2\log(\log\ \mathrm{Rs})}, \tag{36}$$

and so on. Alternatively, a Newton method can be used to obtain δ_1. We can now write the wall shear as

$$\left.\frac{\partial \tilde{u}_0}{\partial \tilde{Y}}\right|_{\tilde{Y}=0} = K(t,s) = \lambda_1^2 U \cos t |U \cos t|. \tag{37}$$

The major result of this is the formula for the nondimensional wall shear given by

$$\tau_w = \frac{\tau_w^*}{\rho U_\infty^{*2}} = \delta_1^2 \lambda_1^2 U \cos t |U \cos t|. \tag{38}$$

The final results in this section are quite universal, and only differences/particular details will be given in the following sections, where we go on to consider (in a little more detail) the application of these results to two well-established turbulence models, namely the $k-\varepsilon$ (Section 3) and Baldwin–Lomax models (Section 4).

3. $k-\varepsilon$ model

The first model we shall utilize is the $k-\varepsilon$ transport model (See Jones and Launder, [7]). This is a two-equation model, bringing two further functions into the equations, namely $U_\infty^{*2} k$, the turbulent kinetic energy, and $U_\infty^{*2}\omega\varepsilon$, the dissipation rate. The nondimensional eddy viscosity is given by

$$\nu_t = c_\mu \frac{k^2}{\varepsilon}\mathrm{Rs}, \tag{39}$$

with two additional transport equations to close the problem, (assuming here $\delta \ll 1$) namely

$$\frac{\partial k}{\partial t} = \frac{\partial}{\partial Y}\left(\frac{\nu_e}{\sigma_k}\frac{\partial k}{\partial Y}\right) P - \varepsilon, \tag{40}$$

$$\frac{\partial \varepsilon}{\partial t} = \frac{\partial}{\partial Y}\left(\frac{\nu_e}{\sigma_\varepsilon}\frac{\partial}{\partial Y}\right) + c_{1\varepsilon}\frac{\varepsilon}{k}P - \upsilon_{2\varepsilon}\frac{\varepsilon^2}{k}, \tag{41}$$

where

$$P = \nu_t\left(\frac{\partial u}{\partial Y}\right)^2. \tag{42}$$

and where $c_\mu, \sigma_k, \sigma_\varepsilon, c_{1\varepsilon}$ and $c_{2\varepsilon}$ are constants of the model. Two sets of constants were used in this study, namely those of Jones and Launder [7]

$$c_\mu = 0{\cdot}09, \quad \sigma_k = 1{\cdot}0, \quad \sigma_\varepsilon = 1{\cdot}3, \quad c_{1\varepsilon} = 1{\cdot}44, \quad c_{2\varepsilon} = 1{\cdot}92, \tag{43}$$

and those proposed by Chien [30]

$$c_\mu = 0{\cdot}09, \quad \sigma_k = 1{\cdot}0, \quad \sigma_\varepsilon = 1{\cdot}3, \quad c_{1\varepsilon} = 1{\cdot}35, \quad c_{2\varepsilon} = 1{\cdot}80. \tag{44}$$

The differences in constants are due to the model being correlated for different types of flows, in particular Jones and Launder [7] determined the constants for severely accelerating flows. For the $k-\varepsilon$ model, we are required to solve (6), together with (39)–(42). As in the previous section, to $O(\delta)$ we find (6) leads to (12), but with

$$\nu_e = 1 + \nu_t = 1 + c_\mu\,\mathrm{Rs}\frac{k^2}{\varepsilon}, \tag{45}$$

As before, we find a double-layer structure. In the inner layer we scale according to (16) together with

$$k = \delta_4\hat{k}, \qquad \varepsilon = \delta_5\hat{\varepsilon}, \tag{46}$$

and we assume the eddy-viscosity is $O(1)$ in this layer, as are all terms involving $\hat{k}$ and $\hat{\varepsilon}$ in the above, yielding the following relationships

$$\delta_4 = \delta_2^{-2}\,\mathrm{Rs}^{-1}, \qquad \delta_5 = \delta_2^{-4}\,\mathrm{Rs}^{-1}, \tag{47}$$

with δ_2 described by (16), and δ_1 by (35).

To leading order of the three transport equations (12), (40) and (41) all become quasi-steady, *i.e.*

$$\frac{\partial}{\partial \widetilde{Y}}\left[\left(1 + c_\mu\frac{\hat{k}^2}{\hat{\varepsilon}}\right)\frac{\partial \tilde{u}_0}{\partial \widetilde{Y}}\right] = 0, \tag{48}$$

$$\frac{\partial}{\partial \widetilde{Y}}\left[\frac{1}{\sigma_k}\left(1 + c_\mu\frac{\hat{k}^2}{\hat{\varepsilon}}\right)\frac{\partial \tilde{k}}{\partial \widetilde{Y}}\right] + c_\mu\frac{\hat{k}^2}{\hat{\varepsilon}}\left(\frac{\partial \tilde{u}_0}{\partial \widetilde{Y}}\right)^2 - \hat{\varepsilon} = 0, \tag{49}$$

$$\frac{\partial}{\partial \widetilde{Y}}\left[\frac{1}{\sigma_\varepsilon}\left(1 + c_\mu\frac{\hat{k}^2}{\hat{\varepsilon}}\right)\frac{\partial \tilde{\varepsilon}}{\partial \widetilde{Y}}\right] + c_{1\varepsilon}c_\mu\hat{k}\left(\frac{\partial \tilde{u}_0}{\partial \widetilde{Y}}\right)^2 - c_{2\varepsilon}\frac{\hat{\varepsilon}^2}{\hat{k}} = 0. \tag{50}$$

We can now integrate (48) once, to obtain

$$\frac{\partial \tilde{u}_0}{\partial \widetilde{Y}} = \frac{F(\hat{t}, \hat{s})}{1 + c_\mu \frac{\hat{k}^2}{\hat{\varepsilon}}}, \tag{51}$$

(*cf.* (20)). If we now examime the limit $\widetilde{Y} \to \infty$, we expect $\partial \hat{u}/\partial \widetilde{Y} \to 0$, and surmise that $\hat{\varepsilon}/\hat{k}^2 \to 0$, so that the turbulent eddy viscosity, ν_t dominates the laminar viscosity, the asymptotic methods suggest that

$$\tilde{u}_0 = u_1(\hat{t}, \hat{s}) \log \widetilde{Y} + \cdots, \qquad \hat{k} = k_1(\hat{t}, \hat{s}) + \cdots, \qquad \hat{\varepsilon} = \frac{\varepsilon_1(\hat{t}, \hat{s})}{\widetilde{Y}} + \cdots, \tag{52}$$

where

$$k_1 = \sigma_\varepsilon u_1^2 (c_{2\varepsilon} - c_{1\varepsilon}), \tag{53}$$

$$\varepsilon_1 = \sqrt{c}_\mu \sigma_\varepsilon |u_1^3| (c_{2\varepsilon} - c_{1\varepsilon}), \tag{54}$$

which are entirely consistent with the Section 2 results. This shows (again) the natural occurrence of the 'log law' in the velocity profile. We now consider the outer layer ($\tilde{y} = O(1)$) wherein the velocity is equal to that of the freestream to leading order and we scale variables according to

$$u = U \cos t + \delta_1 \tilde{u}_0 + \cdots, \quad \hat{k} = \delta_6 k, \qquad \hat{\varepsilon} = \delta_7 \varepsilon, \tag{55}$$

other quantities scaling as in Section 2. If we now substitute the above in (12), (40)–(42), and balance as many terms as possible to leading order, we find

$$\delta_6 = \delta_7 = \delta_2^{-2}\, \mathrm{Rs}^{-1}, \tag{56}$$

and the leading order equations become

$$\frac{\partial \tilde{u}_0}{\partial t} = \frac{\partial}{\partial \tilde{y}} \left[c_\mu \frac{\tilde{k}^2}{\tilde{\varepsilon}} \frac{\partial \tilde{u}_0}{\partial \tilde{y}} \right], \tag{57}$$

$$\frac{\partial \tilde{k}}{\partial t} = \frac{\partial}{\partial \tilde{y}} \left[\frac{c_\mu}{\sigma_k} \frac{\tilde{k}^2}{\tilde{\varepsilon}} \frac{\partial \tilde{k}}{\partial \tilde{y}} \right] + c_\mu \frac{\tilde{k}^2}{\tilde{\varepsilon}} \left(\frac{\partial \tilde{u}_0}{\partial \tilde{y}} \right)^2 - \tilde{\varepsilon}, \tag{58}$$

$$\frac{\partial \tilde{\varepsilon}}{\partial t} = \frac{\partial}{\partial \tilde{y}} \left[\frac{c_\mu}{\sigma_\varepsilon} \frac{\tilde{k}^2}{\tilde{\varepsilon}} \frac{\partial \tilde{\varepsilon}}{\partial \tilde{y}} \right] + c_{1\varepsilon} c_\mu \tilde{k} \left(\frac{\partial \tilde{u}_0}{\partial \tilde{y}} \right)^2 - c_{2\varepsilon} \frac{\tilde{\varepsilon}^2}{\tilde{k}}. \tag{59}$$

Matching the inner and outer velocities, we are led to conclude

$$u_1 = U \cos t. \tag{60}$$

The final result is that we must have $\lambda_1^2 = \sqrt{c_\mu} \sigma_\varepsilon (c_{2\varepsilon} - c_{1\varepsilon})$. Note that in the above we have (implicitly) relaxed the assumption (iii) on Section 2 *i.e.* (15), although this condition is valid

at the outer edge of the sublayer, *i.e.* as $\widetilde{Y} \to \infty$. We shall later (Section 5) consider numerical results arising from this section.

4. The Baldwin–Lomax model

The second turbulence model to be used here is the Baldwin–Lomax [8] model, which is a two-layer algebraic eddy viscosity model. The model is based on that of Cebeci *et al.* [31], and has the great advantage over most mixing-length models that it does not require definition of the 'edge' of the boundary layer. The eddy viscosity ν_t is given by

$$\nu_t = \begin{cases} (\nu_t)_{\text{inner}} & n \leqslant n_c, \\ (\nu_t)_{\text{outer}} & n \geqslant n_c, \end{cases} \tag{61}$$

where n_c is the smallest value of n at which $(\nu_t)_{\text{inner}}$ and $(\nu_t)_{\text{outer}}$ are equal. In the inner region the Prandtl-van Driest formulation is used

$$(\nu_t)_{\text{inner}} = l^2 |\nabla \vee \mathbf{u}|, \tag{62}$$

where

$$l = kn\left[1 - \exp\left(\frac{-n^+}{A^+}\right)\right], \tag{63}$$

and

$$n^+ = \frac{\rho_w u_\tau n}{\mu_w} = \frac{\sqrt{\rho_w \tau_w}\, n}{\mu_w}, \tag{64}$$

with the constant $A^+ = 26$. This, like all constants in the model, was calculated by Baldwin and Lomax [8], requiring agreement with the Cebeci *et al.* [31] formulation for incompressible, constant-pressure boundary layers. For the outer region, the eddy viscosity is given by

$$(\nu_t)_{\text{outer}} = KC_{cp} F_{\text{wake}} F_{\text{Kleb}}(n), \tag{65}$$

where $K = 0{\cdot}0168$ is the Clauser constant, and $C_{cp} = 1{\cdot}6$ is an additional constant. F_{wake} is given by

$$F_{\text{wake}} = \text{the smaller of } \left\{ \begin{array}{c} n_{\max} F_{\max} \\ \frac{C_{\text{wk}} n_{\max} u_{\text{dif}}^2}{F_{\max}} \end{array} \right\}, \tag{66}$$

where $C_{\text{wk}} = 0{\cdot}25$ is a constant and where $n_{\max}$ and $F_{\max}$ are determined from the function

$$F(n) = n|\nabla \wedge \mathbf{u}|\left[1 - \exp\left(\frac{-n^+}{A^+}\right)\right] \tag{67}$$

with $F_{\max}$ being the maximum value of $F(n)$, and $n_{\max}$ being the value of n at which this maximum occurs. The function $F_{\text{Kleb}}(n)$ is the Klebanov intermittency factor, introduced to

ensure the eddy viscosity tends to zero in a regular manner far from the body, thus ensuring the flow tends to that of the freestream, with

$$F_{\text{Kleb}}(n) = \left[1 + 5.5\left(\frac{C_{\text{Kleb}}n}{n_{\max}}\right)^6\right]^{-1}, \tag{68}$$

where the constant $C_{\text{Kleb}} = 0{\cdot}3$. The quantity u_{dif} is the difference between the maximum and minimum total velocity in the profile (*i.e.* at a fixed s station)

$$u_{\text{dif}} = (|\mathbf{u}|)_{\max} - (|\mathbf{u}|)_{\min}. \tag{69}$$

4.1. Leading-order solution

Here, initially we shall again just point out the (minor) differences with the analysis of Section 2. We shall assume that the inner eddy viscosity law is valid throughout the inner ($\widetilde{Y} = O(1)$) layer; this can be shown to be generally correct *a posteriori*. In this region we merely replace (20) with

$$\frac{\partial \tilde{u}_0}{\partial \widetilde{Y}} = \frac{K(t,s)}{1 + \lambda_1^2 \widetilde{Y}^2 \left|\frac{\partial \tilde{u}_0}{\partial \widetilde{Y}}\right| \left[1 - \exp\left(-\lambda_2 \tilde{Y} \left|\frac{\partial \tilde{u}_0}{\partial \widetilde{Y}}\right|^{1/2}_{\widetilde{Y}=0}\right)\right]^2}, \tag{70}$$

the primary difference being the modification of the mixing length (in line with the standard Baldwin–Lomax model) which is therefore a relaxation of the constraint (iii) in Section 2; this has little effect on the remaining results of Section 2.

Solving the problem throughout the whole of the boundary layer would obviously require a numerical approach; we can, however, confirm that the Klebanov intermittency factor ensures the velocity decays to that of the free-stream in the outer limit $\tilde{y} \to \infty$, where the effective viscosity takes the form

$$\nu_e = 1 + \delta_1^2 \,\text{Rs}\,\xi(\tilde{y}_{\max})[1 + \eta(\tilde{y}_{\max})\tilde{y}^6]^{-1}, \tag{71}$$

where ξ and η are functions of $\tilde{y}_{\max}$, and which encompass all the constants of the model and the functions such as F_{wake}, etc.

As we have already discussed, in the outer layer $\nu_t \gg 1$, but as the eddy viscosity decays as $\tilde{y} \to \infty$, there must be a breakdown when $\nu_t = O(1)$, although this is likely to be a passive breakdown, and is unlikely to affect the flow significantly. The laminar viscosity doubly ensures the proper solution asymptote in the freestream.

Also noteworthy is the limit as $t \to \frac{1}{2}\pi$, (or more generally $t \to \frac{1}{2}(2m+1)\pi$, m integer) since this is where the flow reverses its direction of motion on the surface of the cylinder (and indeed in the freestream). If we set $\tilde{t} = t - \frac{1}{2}\pi$, then as $\tilde{t} \to 0$ the scales of the inner and outer regions change somewhat. In the latter case, the appropriate scale appears to be

$$Y = O\left(\frac{\log(\tilde{t}^3\,\text{Rs})}{\tilde{t}\,\text{Rs}^{1/2}}\right),$$

implying a thickening of this region around flow reversal time. In the outer region, as $\tilde{t} \to 0$, then

$$\delta_3 \approx \frac{\log(\tilde{t}^3\,\mathrm{Rs})}{\tilde{t}^2\,\mathrm{Rs}^{1/2}}, \tag{72}$$

implying a thinning of this region, but we see flow reversal is achieved in a relatively smooth manner, and does not disrupt the nature of the flow during the rest of the cycle; the numerical results in Section 5 confirm this.

4.2. Higher-order terms, including steady streaming

For steady streaming in the laminar case inertia terms must play a role in (6). We may show this also to be necessary for the turbulent case using (12), and considering the following integral in terms of the original Y coordinate

$$\int_0^{2\pi}\int_0^{Y}\left[U\sin t + \frac{\partial u_0}{\partial t}\right]\mathrm{d}Y\;\mathrm{d}t = 0, \tag{73}$$

(assuming periodicity in time). Therefore, for general Y from (12)

$$\int_0^{2\pi}\left[\nu_e(Y,t)\frac{\partial u_0}{\partial Y} - \left.\frac{\partial u_0}{\partial Y}\right|_{Y=0}\right]\mathrm{d}t = 0. \tag{74}$$

Since $\nu_e(T,t) > 0$, u_0 can have no component independent of t. Hence inertia terms are vital for the generation of steady streaming, just as in the laminar case.

In the inner region, inspection of (6) suggests a sequence of terms of $O(\delta_1^3\,\mathrm{Rs})$, $O(1)$, $O(\delta_1)$, $O(\delta)$, etc. We have considered the $O(\delta_1^3\,\mathrm{Rs})$ terms previously, whilst if we inspect the $O(1)$ terms we find notionally just one term, that of the leading order pressure $-U\sin t$. This must clearly be balanced by another term, which must be an intermediate term in the u expansion. This suggests some terms given in the expansion below, while other terms can be justified *a posteriori*

$$\begin{aligned} u \;&=\; \delta_1\tilde{u} = \delta_1\{\tilde{u}_0 + O(\delta_1) + \delta_1^{-3}\,\mathrm{Rs}^{-1}\tilde{u}_1 + \delta_1^{-2}\,\mathrm{Rs}^{-1}\tilde{u}_2 \\ &\quad + O(\delta_1^{-1}\,\mathrm{Rs}^{-1}) + \delta\delta_1^{-3}\,\mathrm{Rs}^{-1}\tilde{u}_3 + \cdots\}. \end{aligned} \tag{75}$$

For brevity in what follows, it is useful to define

$$\alpha = \lambda_2\left|\frac{\partial\tilde{u}_0}{\partial\widetilde{Y}}\right|^{1/2}_{\widetilde{Y}=0}.$$

The 'solution' to the quadratic equation (70) may be written

$$\frac{\partial\tilde{u}_0}{\partial\widetilde{Y}} = \kappa\frac{[1+4\lambda_1^4\widetilde{Y}^2(1-\exp(-\alpha\widetilde{Y}))^2|U\cos t|^2]^{1/2}-1}{2\lambda_1^2\widetilde{Y}^2(1-\exp(-\alpha\widetilde{Y}))^2}, \tag{76}$$

and so (see (22) also),

$$\tilde{u}_0 \to U\cos t\log\tilde{Y} + K_0^*(t,s) + \cdots \quad \text{as } \widetilde{Y}\to\infty, \tag{77}$$

where $K_0^*(t,s)$ is periodic in time (with zero mean) on account of the properties of (74). Higher-order matching between the $\tilde{y}$ and $\widetilde{Y}$ regions then requires a slight (higher-order) adjustment to our definition of (35) leading to

$$1+\delta_1\left\{\frac{A_0}{U\cos t}-\frac{K_0^*}{U\cos t}-\log(\mathrm{Rs}\delta_1^2\right\}=0, \tag{78}$$

(where $u_0^*\to U\cos t\log\tilde{y}+A_0(t,s)+\cdots$ as $\tilde{y}\to 0$) since A_0 and K_0^* are both determined independently, from the outer and inner layers respectively. However this re-definition of δ_1 has little effect on the actual evalution of δ_1, (see (35), (36)). In some ways the most profound effect is that the derivative $\frac{\partial}{\partial t}$ leads to additional terms of the form

$$\frac{\widetilde{Y}}{\delta_1}\frac{\partial\delta_1}{\partial t}\frac{\partial}{\partial\widetilde{Y}}$$

in the inner layer and

$$\frac{\tilde{y}}{\delta_1}\frac{\partial\delta_1}{\partial t}\frac{\partial}{\partial\tilde{Y}}$$

in the outer layer, (together with the $\partial\delta_1/\partial t$ terms that must obviously occur).

Further, we note that additional, even higher-order terms are likely to appear in (78) above. Finally, with respect to this particular point, we note that $\partial\delta_1/\partial t=O(\delta_1^2)$. Although the next term in the u expansion is likely to be $O(\delta_1^2)$, this term turns out to be inconsequential for our purposes. Instead we turn out attention to the $O(\delta_1^{-2}\ \mathrm{Rs}^{-1})$ term in the u expansion, obtained through consideration of the $O(1)$ terms in (8). (Although these are smaller than the previously neglected $O(\delta_1^2)$ Rs), some higher-order terms may be determined independently of lower-order terms.) We may regard this solution, therefore, as developing in the form of parallel infinite series. With details omitted for the sake of brevity, after some algebra we find the following series solution for $\tilde{u}$ in the limit as $\widetilde{Y}\to\infty$

$$\begin{aligned}
\tilde{u}\ =\ & U\cos t\log\widetilde{Y}+K_0^*(t,s)+\cdots+O(\delta)\\
&+\delta_1^{-3}\,\mathrm{Rs}^{-1}\left\{\kappa\frac{\tan t}{2\lambda_1^2}\widetilde{Y}+\frac{K_1(t,s)}{2\lambda_1^2|U\cos t|}\log\widetilde{Y}+K_1^*(t,s)+\cdots\right\}\\
&+\delta_1^{-2}\,\mathrm{Rs}^{-1}\left\{-\kappa\frac{\tan t}{2\lambda_1^2}\widetilde{Y}+(\log\widetilde{Y}-2)+\frac{K_2(t,s)}{2\lambda^2|U\cos t|}\log\widetilde{Y}\right.\\
&\qquad\left.+\frac{1}{2\kappa\lambda_1^2U\cos t}\frac{\partial K_0^*}{\partial t}\widetilde{Y}+K_2^*(t,s)+\cdots\right\}+O(\delta_1^{-1}\,\mathrm{Rs}^{-1})\\
&+\delta\delta_1^{-3}\,\mathrm{Rs}^{-1}\left\{-\frac{\sec t\tan^2 t}{16\lambda_1^4U}\widetilde{Y}^2-\frac{\kappa\cos t}{2\lambda_1^2}\frac{\mathrm{d}U}{\mathrm{d}s}\widetilde{Y}\right.\\
&\qquad\left.-\frac{K_1(t,s)\sec^2 t\tan t}{8\lambda_1^4U^2}\widetilde{Y}+\cdots\right\},
\end{aligned}\tag{79}$$

The first occurrence of the steady streaming is seen in the final order detailed above, in particular in the term involving $\mathrm{d}U/\mathrm{d}s$. However it is also important to point out that a number

of the terms in the above are independent of U, and hence also of s and indeed of the body geometry in general, and this suggests these results must be treated with some caution, and that a breakdown/limitation of the turbulence model itself may be suggested. Certain of the terms above also predict a discontinuity of velocity along the line of symmetry (for example in the case of flow past a circular cylinder), and singularities of solution at certain times during the cycle, factors again indicating that some caution must be exercised when interpreting these higher-order results.

Returning to the outer layer steady-streaming effects will first arise from the $O(\delta\delta_1)$ terms in the outer u expansion, and these lead to the following (symbolic) solution as $\tilde{y} \to 0$.

$$\bar{u}_1^* = a_1(t,s)\log\tilde{y} + a_2(t,s) + a_3(t,s)\tilde{y}\log\tilde{y} + a_4(t,s)\tilde{y} + a_5(t,s)\tilde{y}^2(\log\tilde{y})^2 + \cdots, \tag{80}$$

where $a_3(t,s)$ contains a term of the form

$$\frac{\kappa\cos t}{\lambda_1^2}\frac{\mathrm{d}U}{\mathrm{d}s}$$

and a_4 a term of the form

$$-\frac{5\kappa\cos t}{2\lambda_1^2}\frac{\mathrm{d}U}{\mathrm{d}s},$$

both of which imply a nonzero time-mean component. Note that higher-order terms ensure a correct match between the inner and outer solutions. We find from this a steady velocity component of $O(\delta\delta_1^{-3}\,\mathrm{Rs}^{-1})$ in the inner layer and $O(\delta_1\delta)$ in the outer layer. We note again that for the particular case of the circular cylinder (for which $U(s) = 2\sin s$), elements of the steady-streaming solution take the form $\mathrm{sign}\{\sin s\}\cos s$. This implies a discontinuity in the steady-streaming velocities conceivably leading to an impact at the line of symmetry (although ratification of this would require full numerical solution). In the laminar case there is also a collision of the steady boundary layers along $s = 0, \pi$, but the outer dubious facets of the turbulent solution (notably the singularities and other discontinuities) are not present, suggesting that the turbulence model is inadequate at this high order. Indeed, the model is likely to be inappropriate for the numerical evaluation of these higher-order terms, but is adequate for the evaluation of the oscillatory terms (Cobbin *et al.* [6]).

Progress with the Baldwin–Lomax model to still higher orders proves prohibitive due to algebraic difficulties (aggravated by the occurrence of the terms arising from $\partial\delta_1/\partial t$, as discussed earlier in this section). We note that the overall structure of the solution involves three notionally independent (small) parameters, namely δ, Rs^{-1} and δ_1. Although the latter two are linked, and it would be feasible to assign a magnitude to δ in terms of one of the other parameters, with our approach three sets of inter-related series emerge. An analogous (but simpler) situation arises in the far downstream analysis of the laminar boundary layer on an axisymmetric body, as studied by Glauert and Lighthill [32], Stewartson [33] and Bush [34].

We further note that there may well be a further layer, thicker still than the outer layer, caused by the steady streaming. Simple order-of-magnitude arguments suggest this could be given by

$$\tilde{y} = O\left(\left(\frac{\delta_1}{\delta^2}\right)^{1/8}\right) \quad \text{if } \delta_1^{11/4}\,\mathrm{Rs}\delta^{3/4} > 1, \quad \text{or}$$

$$\tilde{y} \;=\; O(\delta^{-1/2}\,\mathrm{Rs}^{-1/2}\delta^{-1}) \quad \text{if } \delta_1^{11/4}\,\mathrm{Rs}\delta^{3/4} < 1.$$

However, affirmation of this point is not possible without detailed, numerical confirmation of the higher-order terms within the $\tilde{y} = O(1)$ layer, (also involving the intermittency factor) and this is prohibited in part by the various solution discontinuities/singularities that emerge.

A similar investigation involving the evalution of higher-order terms using the $k-\varepsilon$ model was found less amenable to analysis of this kind (because of its greater complexity) and equivalent progress has not been made.

5. Numerical results, comparisons and conclusions

Since curvature effects may be ignored to leading order, the solutions we have obtained are applicable to an oscillating flow past a flat plate, for which we merely put $U = 1$. Thus we are able to compare with previous results for the flat plate directly, and we consider mainly the results of Cobbin *et al.* [6], which were obtained numerically using the Baldwin–Lomax mixing-length turbulence model, including the intermittency factor, using a logarithmically spaced transverse grid to improve accuracy. The results of Cobbin *et al.* predict the onset of turbulence at about $\mathrm{Rs} \approx 10^5$, and they should provide validation of the $\mathrm{Rs} \to \infty$ asymptotics in this study (although we do *not* expect the current study to model the transition process).

The only difference between the results for the Baldwin–Lomax model and the $k-\varepsilon$ model is in the constants (in fact, $\lambda_2^2 = 0{\cdot}16$, and $\sqrt{c_\mu}\sigma_\varepsilon(c_{2\varepsilon} - c_{1\varepsilon}) = 0{\cdot}1872$ for the constants of Jones and Launder, [7] and $\sqrt{c_\mu}\sigma_\varepsilon(c_{2\varepsilon} - c_{1\varepsilon}) = 0{\cdot}1755$ for those of Chien, [30]), the different results arising from the different empirical analyses of these authors. For two turbulence models of such different forms, this is a gratifying result. We can thus calculate the variation of the wall shear throughout an entire cycle. When so doing, we must bear in mind that because of multiple nested logarithms involved in the calculation of δ_1 the series may be very slow to decay and it is very difficult to say at what value of (finite) Rs the asymptotics will give a good approximation to the numerical results. In Figure 1 we have plotted the wall shear against time for the highest value of Rs considered by Cobbin *et al.* [6], namely, $\mathrm{Rs} = 10^7$. We note the qualitative similarities with the results of Spalart and Baldwin [3]. From this graph we see that the two curves have a similar phase, with the numerical values having a slightly larger amplitude than our asymptotic results. It must be remembered that only the first terms in the series were taken and so this level of accuracy is reasonably acceptable. There are, however, two jumps in the curves for the numerical case; these are due to the eddy viscosity switching between the two expressions for F_{wake}. This switching occurs close to the time of flow reversal and is due to the $U_{\mathrm{DIF}}^2 = U^2\cos^2 t$ term becoming relatively small as $t \to \frac{1}{2}(2m+1)\pi$.

We can also determine the variation of the friction factor, f_w, with the steady streaming Reynolds number, Rs. For the laminar case, $f_w = 2\mathrm{Rs}^{-1/2}$. Here f_w is given by

$$f_w = \max_{0\leqslant t\leqslant 2\pi}\left\{\frac{\tau_w^*}{\frac{1}{2}\rho^* U_\infty^{*\,2}}\right\} = 2\delta_1^2\lambda_1^2, \tag{81}$$

and

$$f_w = \max_{0\leqslant t\leqslant 2\pi}\left\{\frac{\tau_w^*}{\frac{1}{2}\rho^* U_\infty^{*\,2}}\right\} = 2\delta_1^2\mathrm{Rs}^{-1}\sqrt{c_\mu}\sigma_\varepsilon(c_{2\varepsilon} - c_{1\varepsilon}), \tag{82}$$

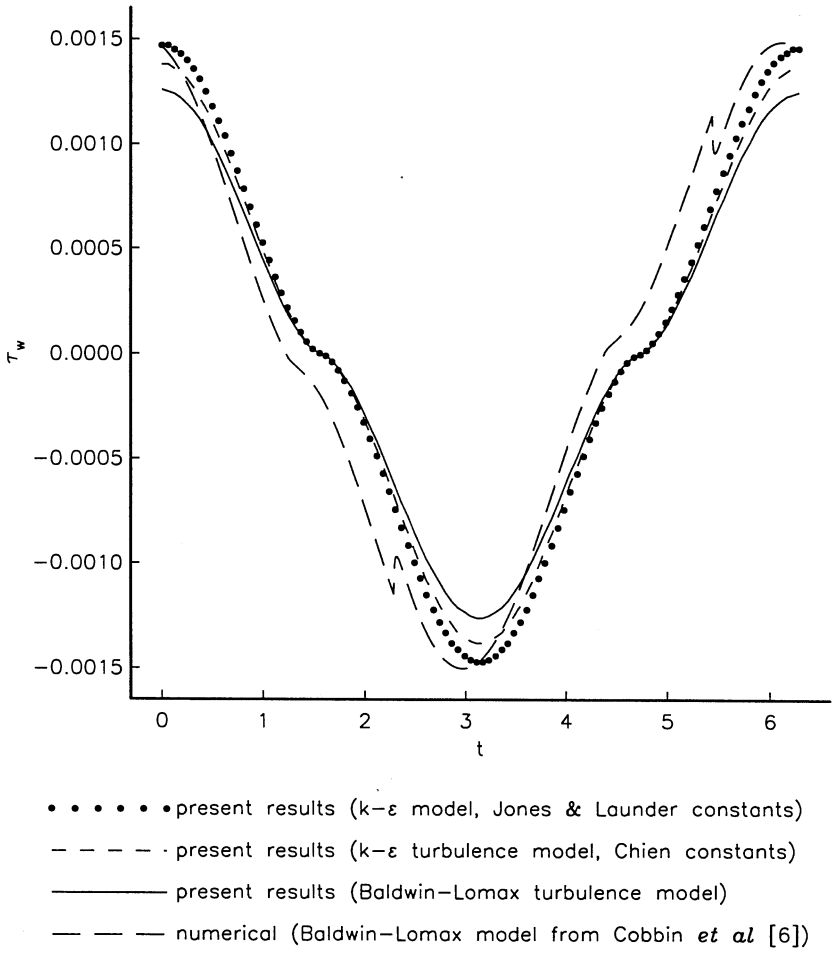

Figure 1. Plot of wall shear against time, Rs $= 10^7$.

for the two turbulence models. The variation of f_w with Rs is shown in Figure 2. The dashed line represents results obtained from the Baldwin–Lomax model, while the solid lines are those of the $k - \varepsilon$ model, with the constants of Jones and Launder [7] (upper curve) and Chien [30] (lower curve). From this figure we can see the effect of transition on the results of Cobbin *et al.* [6], namely the jump in the values at Rs $\approx 2 \times 10^5$ as we would expect. There is, however, general convergence of other results with our asymptotic results as Rs $\to \infty$. We find that the intersection of the present Baldwin–Lomax model turbulent curve with the laminar curve occurs at roughly Rs $\approx 1{\cdot}5 \times 10^5$, which therefore gives a remarkably good (somewhat fortuitous) agreement with the point of transition.

We can also obtain, to leading order, the pseudo-displacement thickness δ^*, defined by

$$\delta^* = \int_0^\infty [u - U \cos t] \, \mathrm{d}Y. \tag{83}$$

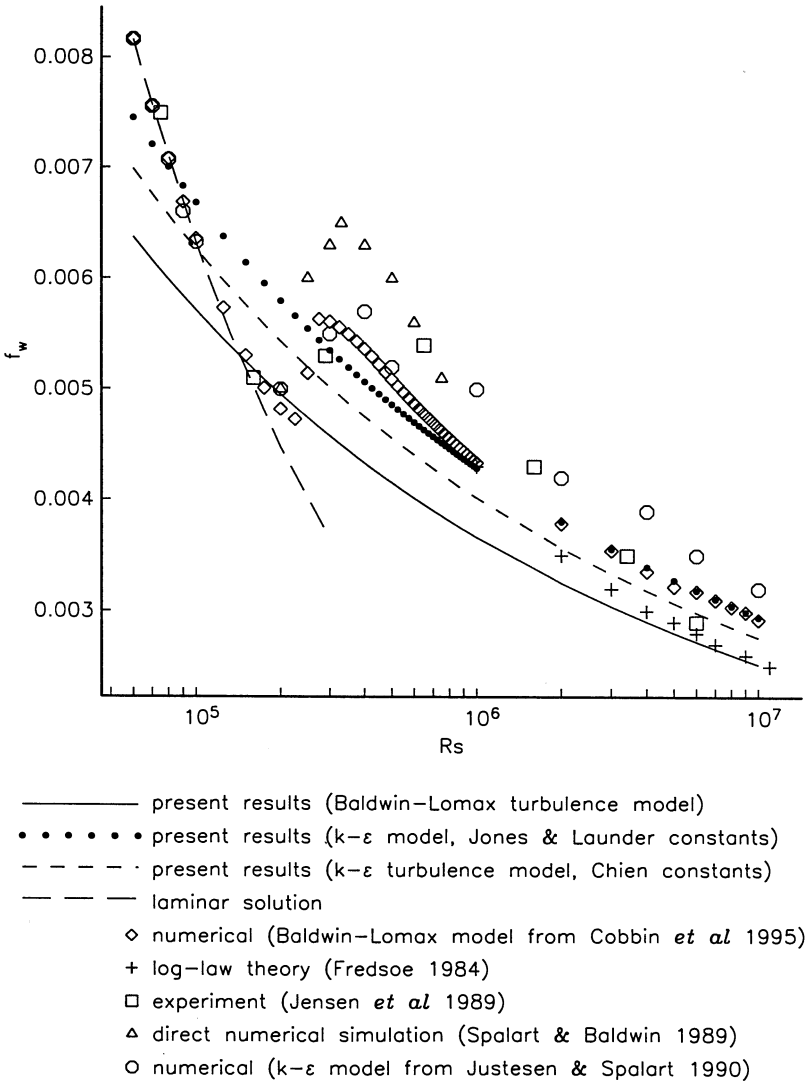

Figure 2. Plot of friction factor against Rs.

If we now take the leading order terms of (6), we have (12), which can be integrated with respect to Y so that

$$\int_0^\infty \frac{\partial}{\partial t}(u - U\cos t)\,\mathrm{d}Y = \left[\nu_e \frac{\partial u}{\partial Y}\right]_0^\infty = -\left.\frac{\partial u}{\partial Y}\right|_{Y=0}, \tag{84}$$

which implies

$$\frac{\partial \delta^*}{\partial t} = -\left.\frac{\partial u}{\partial Y}\right|_{Y=0}. \tag{85}$$

For the circular cylinder problem, the force depends on the shear stress distribution and the pseudo-displacement thickness and can thus be simply obtained. The contribution to the force due to pressure F_p is given by

$$F_p = \frac{2}{\delta}\cos s \sin t + 2\sin^2 s \cos^2 t, \tag{86}$$

and due to shear stress F_s is given by, for the Baldwin–Lomax model

$$F_s = 4\delta_1^2\lambda_1^2 \sin s \cos t |\sin s \cos t|. \tag{87}$$

The force on a cylinder is normally described by the Morison *et al.* [35] formula, with components in phase with the velocity (drag) and in phase with acceleration (inertia)

$$F = \rho a C_D |U| U + \pi\rho a^2 C_M \frac{\mathrm{d}U}{\mathrm{d}t^*}. \tag{88}$$

The inertia coefficient C_M is very close to its potential flow of 2 for attached flows in the case of a circular cylinder, and here we are only concerned with the drag or damping force defined by the drag coefficient.

The drag coefficient on the cylinder is then given by (*e.g.* Sarpkaya, [14])

$$C_D = -\frac{3}{4}\int_0^{2\pi} (C_s + C_p)\cos t \, \mathrm{d}t, \tag{89}$$

where

$$C_s = \int_0^{2\pi} F_s \sin s \, \mathrm{d}s = \tfrac{32}{3}\delta_1^2\lambda_1^2 \cos t |\cos t|, \tag{90}$$

and

$$C_p = \int_0^{2\pi} F_p \cos s \, \mathrm{d}s = \frac{2\pi}{\delta}\sin t. \tag{91}$$

This gives, for the Baldwin–Lomax model

$$C_D = -\tfrac{64}{3}\lambda_1^2\delta_1^2. \tag{92}$$

The same procedure for the $k-\varepsilon$ model gives

$$C_D = -\tfrac{64}{3}\sqrt{c_\mu}\sigma_\varepsilon(c_{2\varepsilon} - c_{1\varepsilon})\delta_1^2 \ \mathrm{Rs}^{-1}. \tag{93}$$

These curves are shown in Figure 3.

The expressions for τ_w can be generalised for any external flow $U_e(s.t)$ (replacing $U\cos t$ in the above), and with an nondimensionalisation such that $\max_{s,t}|U_e(s,t)| = 1$ we find (for the Baldwin–Lomax and $k-\varepsilon$ models respectively)

$$\tau_w = \delta_1^2\lambda_1^2 U_e(s,t)|U_e(s,t)|, \tag{94}$$

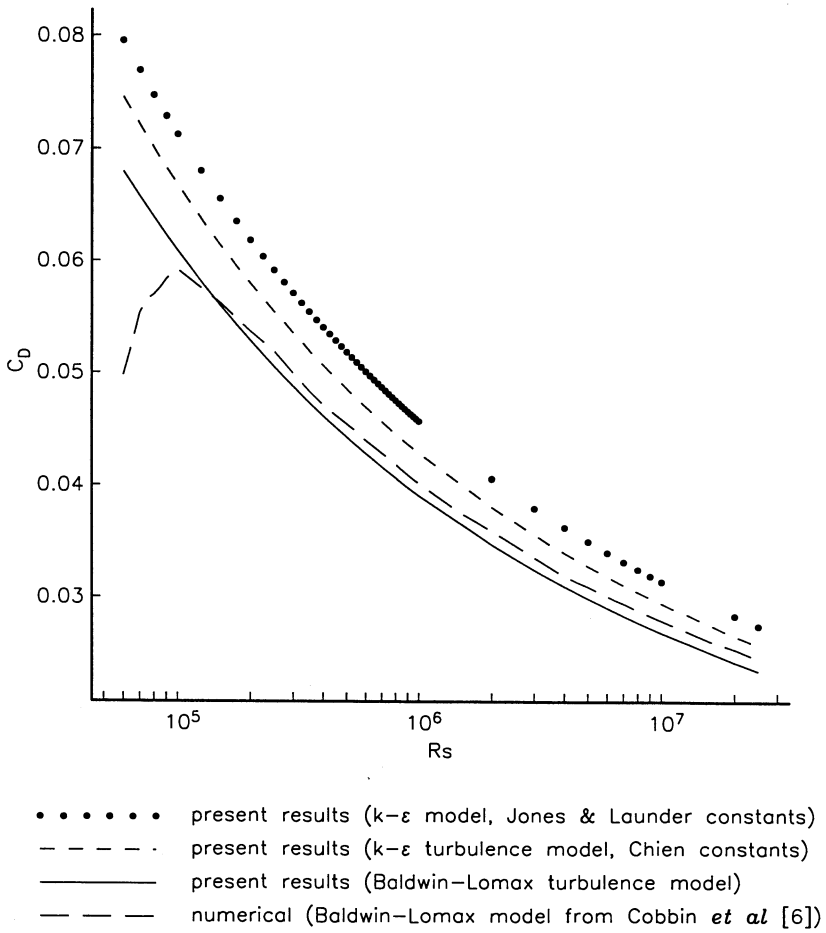

Figure 3. Plot of drag coefficient against Rs.

and

$$\tau_w = \delta_1^2 \,\mathrm{Rs}^{-1} \sqrt{c_\mu}\sigma_\varepsilon (c_{2\varepsilon} - c_{1\varepsilon}) U_e(s,t)|U_e(s,t)|. \tag{95}$$

Taking, for example, $U_e(s,t) = \frac{2}{3}\cos t + \frac{1}{3}\cos 3t$, we show in Figure 4 the variation of wall shear with time throughout one cycle, comparing with unpublished numerical results kindly provided by A. Cobbin; the agreement is reasonable. Note that the 'wiggles' in Figures 1 and 4 in the numerical results (rather than the asymptotic results which have been derived here) are likely to be caused by changes in the viscosity law, described by (61), around times when flow reversal occurs.

To conclude, therefore, the turbulent oscillatory boundary layer on a circular cylinder has been analysed in the limit of large Reynolds number (or more specifically, steady-streaming Reynolds number Rs). Although the entire velocity profile across the boundary layer has not been calculated in detail, nontheless it is possible to obtain important analytic results (including shear stress and displacement thickness) despite this, on the basis of just the three basic assumptions made in Section 2 (one of which can be relaxed, anyway). The results are found to be entirely consistent with both the $k - \varepsilon$ and Baldwin–Lomax models, which yield very

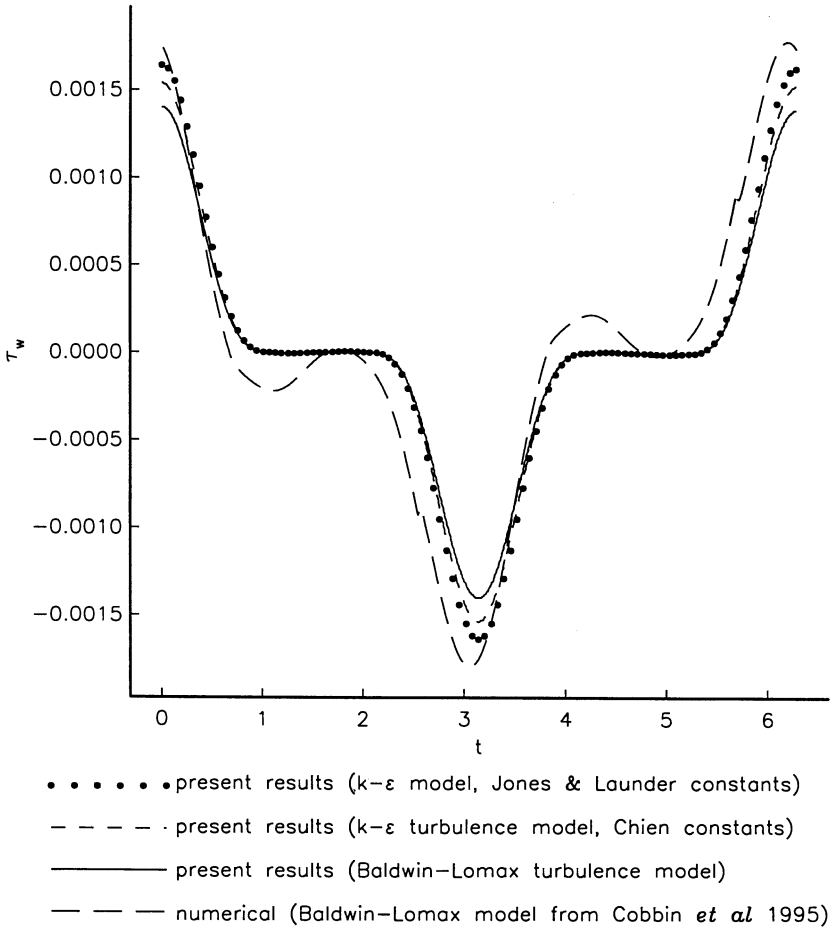

Figure 4. Plot of wall shear against time for $U_e = \frac{2}{3}\cos t + \frac{1}{3}\cos 3t$ with $\mathrm{Rs} = 10^7$.

similar results for basic flow properties, differing merely by the choice of the multiplicative constants.

For cylinder flows, to leading order the local flow is taken to be equivalent to the oscillatory flow over a flat plate and results have been shown to be consistent with previous numerical work. We note that in the case of a flat plate, we merely need to set $U = 1$ in our results, and then there is no longer any need for the requirement that $\delta \ll 1$, just that $\mathrm{Rs} \gg 1$.

For cylinder flows, higher-order, including steady-streaming effects for the Baldwin–Lomax model have been analysed. However, the discontinuities and singularities resulting from the Baldwin–Lomax model suggest the turbulence model may be inadequate at these higher orders. Higher-order (including steady-streaming) effects will also occur through displacement effects of the boundary layer, but these will be of higher order than those considered here. However leading-order results show reasonable agreement with previous experimental and computational results (of the oscillatory flow).

Overall, there is some similarity of the solution structure with previous (asymptotic) studies on steady turbulent flows (for example Mellor, [23] and Bush and Fendell, [24]), and also intriguingly with the far downstream solution for the boundary layer on a body of revolution. It is worth stressing that most of this analysis is also applicable to flow past general-shaped,

smooth cylinders/surfaces, in arbitrary time-varying (zero-mean) flows, of the form studied numerically by Cobbin *et al.* [36]. An obvious extension to this work would be the use of more modern, sophisticated closure models, such as the Reynolds stress transport equations (Launder *et al.* [37]), although the associated system of equations would inevitably be of higher order, but could perhaps lead to more useful higher-order solutions than those presented here.

Acknowledgment

M. J. Butler is funded through an Engineering and Physical Sciences Research Council studentship, which is gratefully acknowledged.

References

1. G. G. Stokes, On the effect of the internal friction of fluids on the motion of pendulums. *Trans Combr. Phil. Soc.* 9 (1851) 35–48.
2. B. L. Jensen, B. M. Summer and J. Fredsoe, Boundary layers at high Reynolds numbers. *J. Fluid Mech.* 206 (1989) 265–297.
3. P. R. Spalart and B. S. Baldwin, Direct simulation of a turbulent oscillatory boundary layer. In: J.-C. André, J. Consteix, F. Durst, B. E. Launder, F. W. Schmidt and J. H. Whitelaw (eds.), *Turbulent shear Flows* 6. Berlin: Springer (1989) pp. 417–440.
4. J. Fredsoe, The turbulent boundary layer in wave-current motion. *J. Hydraulics Div. ASCE* 110 (1984) 1–37.
5. P. Justesen and P. R. Spalart, Two-equation turbulence modeling of oscillatory boundary layers. *AIAA 28th Aerospace Sciences Meeting* (1990) AIAA paper 90-0496.
6. A. M. Cobbin, P. K. Stansby and P. W. Duck, The hydrodynamic damping force on a cylinder in oscillating, very-high-Reynolds-number flows. *Appl. Ocean Res.* 17 (1995) 291–300.
7. W. P. Jones and B. E. Launder, The prediction of laminarization with a two-equation model of turbulence. *Int. J. Heat and Mass Transfer* 15 (1972) 301–314.
8. B. S. Baldwin and H. Lomax, Thin layer approximation and algebraic model for separated turbulent flows. *AIAA 16th Aerosp. Sci. Meeting* (1978) AIAA paper 78–257.
9. J. T. Stuart, Double boundary layers in oscillatory viscous flow. *J. Fluid Mech.* 24 (1965) 673–687.
10. N. Riley, Oscillating viscous flows. *Mathematika* 12 (1965) 161–175.
11. N. Riley, Oscillatory viscous flows. Review and extension. *J. Inst. Maths. Applics.* 3 (1967) 419–434.
12. G. H. Keulegan and L. H. Carpenter, Forces on cylinders and plates in an oscillating fluid. *J. Res. Nat. Bur. Stand.* 60 (1958) 423–440.
13. T. Sarpkaya, Forces on cylinders and spheres in a sinusoidally oscillating fluid. *J. Appl. Mech* 42 (1975) 32–37.
14. T. Sarpkaya, force on a circular cylinder in a viscous oscillatory flow at low Keulegan–Carpenter numbers. *J. Fluid Mech.* 165 (1986) 61–71.
15. H. Honji, Streaked flow around on oscillating circular cylinder. *J. Fluid Mech.* 107 (1980) 509–520.
16. P. Hall, On the stability of the unsteady boundary layer on a cylinder oscillating transversely in a viscous fluid. *J. Fluid Mech.* 146 (1984) 347–367.
17. K. Kajiura, A model of the bottom boundary layer in water waves. *Bull. Earthquake Res. Inst.* 46 (1968) 75–123.
18. I. Brevik, Oscillatory rough turbulent boundary layers. *J. Waterway, Port and Ocean Division, ASCE* 107 (1981) 175–188.
19. W. T. Bakker, Sand concentration in an oscillatory flow. *Proc. 14th. Conf. Coastal Engineering*. Copenhagen: ASCE (1974) pp. 1129–1148.
20. L. Prandtl, Über die ausgebildete Turbulenz, *Proc. 2nd. Int. Cong. Appl. Mech.*, Zurich (1926) pp. 62–74; translated as Turbulent Flow, *Nat Adv. Comm. Aero., Wash., Tech. Mem.* 435 (1927).
21. I. G. Jonnson and N. A. Carlsen, Experimental and theoretical investigations in an oscillatory turbulent boundary layer. *J. Hydraulic Res.* 14 (1976) 45–60.

22. K. S. Yajnik, Asymptotic theory or turbulent shear flows. *J. Fluid Mech.* 42 (1970) 411–427.
23. G. L. Mellor, The large Reynolds number, asymptotic theory of turbulent Boundary Layers. *Int. J. Engng. Sci.* 10 (1972) 851–873.
24. W. B. Bush and F. E. Fendell, Asymptotic analysis of turbulent channel and boundary-layer flow. *J. Fluid Mech.* 56 (1972) 657–681.
25. J. He, J. Y. Kazakia and J. D. A. Walker, An asymptotic two-layer model for supersonic turbulent boundary layers. *J. Fluid Mech.* 295 (1995) 159–198.
26. A. T. Degani, F. T. Smith and J. D. A. Walker, The three-dimensional turbulent boundary layer near a plane of symmetry. *J. Fluid Mech.* 234 (1992) 329–360.
27. A. T. Degani, F. T. Smith and J. D. A. Walker, The structure of a three-dimensional turbulent boundary layer. *J. Fluid Mech.* 250 (1993) 43–68.
28. A. Neish and F. T Smith, On turbulent separation in the flow past a bluff body. *J. Fluid Mech.* 241 (1992) 443–467.
29. P. W. Duck, The effect of a surface discontinuity on an axisymmetric boundary layer. *Q. J. Mech. Appl. Math.* 37 (1984) 57–74.
30. K.-Y. Chen, Predictions on channel and boundary layer flows with a low-Reynolds-number turbulence model. *AIAA J.* 20 (1982) 33–38.
31. T. Cebeci, A. M. O. Smith and G. Mosinskis, Calculation of compressible adiabatic turbulent boundary layers. *AIAA J.* 8 (1974) 1974–1982.
32. M. B. Glauert and M. J. Lighthill, The axisymmetric boundary layer on a long thin cylinder. *Proc. R. Soc. London* A320 (1955) 188–203.
33. K. Stewartson, The asymptotic boundary layer on a circular cylinder in axial incompressible flow. *Quart. J. Appl. Math.* 13 (1955) 113–132.
34. W. B. Bush, Axial incompressible viscous flow past a slender body of revolution. *Rocky Mount. J. Math.* 6 (1976) 527–550.
35. J. R. Morison, M. P. O'Brien, J. W. Johnson and S. A. Schaaf, The force exerted by surface waves on piles. *Petroleum Trans.* 189 (1950) 149–157.
36. A. M. Cobbin, P. K. Stansby and P. W. Duck, The Viscous Force on Noncircular Cylindrical Bodies in Attached Turbulent Oscillatory Flow (1998). In preparation.
37. B. E. Launder, G. J. Reece and W. Rodi, Progress in the development of a Reynolds stress turbulence closure. *J. Fluid Mech.* 68 (1975) 537–566.